NMDA receptor-dependent dynamics of hippocampal place cell ensembles

Yuichiro Hayashi[1,2*]

[1]Frontier Research Center for Post-genome Science and Technology, Hokkaido University,

Kita-21 Nishi-11 Kita-ku, Sapporo, Japan 001-0021

[2]Institute of Biomedical Sciences, Kansai Medical University, Hirakata, Osaka 573-1010, Japan

Correspondence should be addressed to Yuichiro Hayashi

(email:hayasyui@hirakata.kmu.ac.jp)

Activity patterns of hippocampal neural population gradually change over time when the same event is repeated. This temporal dynamics of population activity may support to retain distinct memories of spatially identical, but temporally different, episodes. However, whether difference in population activity for the same event is principally dependent on time or also dependent on event rate in unit time is unknown. Long-term imaging of hippocampal CA1 neurons of mice was performed during repeated performance in a spatial memory task. Overlap of place cell population was independent of the number of tasks performed in a fixed time period, but it was dependent on the duration between the sessions. This time-dependent change of hippocampal ensemble code was suppressed by the administration of an NMDA receptor antagonist. These results suggested that the gradual change of activity pattern in the hippocampus works as a code for time, and NMDA receptor-dependent synaptic plasticity serves to form the code.

Abbreviations

NMDA, N-methyl-D-aspartate; R-CPP, 3-((R)-2-Carboxypiperazin-4-yl)-propyl-1-phosphonic acid; LTP, long-term potentiation; AAV, adeno-associated virus

Temporal and spatial context of events are fundamental components of episodic memory [1]. The hippocampus has been shown to play an important role in episodic memory formation [2–5]. Place cells in the hippocampus are active in distinct locations in a given space, suggesting that these cells provide spatial context for an episodic memory [6–8]. Although coding for space has been extensively studied, hippocampal coding for time was scarcely studied until recently. A sequence of activity by a set of neurons in the hippocampus is observed in temporally structured tasks in a timescale from hundred milliseconds to minutes [9–11]. For longer timescales ranging from minutes to weeks, population activity of place cells in relation to a given environment dynamically changes over time [12–16]. In particular, for timescales longer than one day, these changes are mainly the result of turnover of active neurons from session to session, and the overlap of active subsets of neurons across different days declines with time [14,15]. Therefore, events occur at the same place but different times are coded differently in the hippocampus, which may be used to store temporal context of episodic memory [12–16]. Moreover, distinct events occurred at short time intervals are more likely to affect the activity of the same neuronal population, suggesting that the rate of overlap of active cells is a neural representation of temporal distance [17]. However, the factor responsible for the temporal dynamics of hippocampal activity is uncertain. One possibility is that speed of changes in the activity pattern is constant, and thus time is the primary determinant of temporal dynamics. Another possibility is that experience modulates the speed of activity changes. In this case, event frequency affects temporal dynamics. To test these hypotheses, time-lapse imaging of calcium activity of mice hippocampal CA1 neurons was performed during repeated performance in a spatial memory task. The overlap of active place cell populations was independent of the number of tasks performed in two recording sessions, but it was dependent on the duration between the sessions. This experience-independent change of hippocampal ensemble code was suppressed by the

administration of 3-((R)-2-Carboxypiperazin-4-yl)-propyl-1-phosphonic acid (R-CPP), an N-methyl-D-aspartate (NMDA) receptor antagonist.

Results

Long-term recording studies have revealed that activity patterns of hippocampal place cells gradually changes, although the same event occurs. Whether time exclusively determines the rate of change in the population activity or experience also affects this rate was tested. Place cell activity in the hippocampal CA1 region was recorded using a combination of a genetically-encoded calcium indicator and fluorescent imaging (Fig. 1A, B). The mouse was head-fixed on a spherical treadmill that allowed it to run freely (Fig. 1A) [18]. A custom virtual reality (VR) system for rodents was used to present spatial cues (Fig. 1A, C, D) [19–22]. A liquid crystal display monitor installed in front of the mouse displayed a computer-generated image of a virtual linear track (Fig. 1A, C, D). Mice were injected an adeno-associated virus (AAV) expressing GCaMP6f into the pyramidal cell layer of the hippocampal CA1 region and then implanted with a glass window. After 2–4 weeks of recovery, mice were trained to obtain a sugar water reward at a hidden goal zone in the virtual linear track (Fig. 1D). Once the mice were proficient at the task (>10 rewards per single 10 min session), activity patterns of the hippocampal CA1 cells were repeatedly measured in the same task with varying task intervals (Fig. 2, 3A). Across all recording sessions (n = 8 recording sites, 7 mice, 172–492 cells per site), activity of the mice and their reward rate did not vary (Supplementary Fig. 1). Approximately one-fourth of cells exhibited location-specific activity, and basic properties of place cell activity such as mean calcium event rate, fraction of cells having a significant place field, spatial information content, number of place fields, and place field width did not change throughout the sessions (Fig. 3B and Supplementary Fig. 2). As described in previous studies, majority of place

cells were only active in a subset of sessions (Fig. 3B) [14,15]. First, the effects of interval between sessions on the recurrence probability of place cell activity from one session to the next session were evaluated. Recurrence probability is defined as the probability for a cell to exhibit a statistically significant place field in one session has also a place field in a subsequent session [15].

Higher probability of recurrence was observed between 1-day interval sessions than 3-day interval sessions (Fig. 3C, *Left*; 0.58 ± 0.020 for 1-day interval; 0.47 ± 0.040 for 3-day interval; $P = 0.0044$, unpaired *t* test). Analysis of time-series data also indicated that recurrence probability was higher between 1-day interval sessions than 3-day interval sessions (Fig. 3C, *Middle*). Then, the effects of task frequency per fixed time on recurrence probability were tested. In the first trial block, mice performed the task every day between the recording sessions (Days 1–4 in Fig. 3A). In the second block, mice did not perform the task between the recording sessions (Days 4–7 in Fig. 3A). In the last block, mice performed the task every day again between the recording sessions (Days 7–10 in Fig. 3A). No significant difference was observed in recurrence probability among these three trial blocks, indicating that task frequency had no detectable effect on the speed of place cell turnover (Fig. 3C *Right*).

Next, the effects of time and task frequency on the day-to-day fluctuation of place field location were evaluated. As shown in Fig. 3D and E, there was no significant difference in place field shift when the interval or task frequency was varied. These results are consistent with previous observations indicating that the place field location of each cell is generally stable over time [14,15,23,24].

Place cell turnover was dependent on NMDA receptors

NMDA receptors have been identified to play a critical role in synaptic plasticity as well as in hippocampal memory [25–27]. Previous studies have shown that inhibition of NMDA receptors

sustain long-term potentiation (LTP) at perforant path-dentate gyrus synapses and promotes retention of hippocampal memory [28–30]. These studies have led to the idea that place cell turnover is also an NMDA receptor-dependent process.

To test this hypothesis, the NMDA receptor antagonist R-CPP was systemically administrated just after the first recording session and daily thereafter for two days (Fig. 4A). The drug administration had no effect on either animal behavior (Supplementary Fig. 3) or place cell properties including mean calcium event rate, fraction of cells having a significant place field, spatial information content, number of place fields, and place field width (Supplementary Fig. 4; n = 5 mice, 207–294 cells per animal for saline; n = 5 mice, 101–263 cells per animal for CPP). Recurrence probability of place cell activity for the 3-day interval was significantly increased in the CPP group compared with the saline group (Fig. 4B; 0.48 ± 0.053 for saline; 0.68 ± 0.056 for CPP, P = 0.032, Mann–Whitney U test). At the same time, no significant difference was observed in the amount of place field shift between the saline and CPP groups (Fig. 4C).

Discussion

Previous studies have shown that active population of CA1 place cells change dynamically over time when the animals are repeatedly exposed to a familiar environment [14,15]. However, it is unclear whether these activity changes are induced by time only or are also affected by experience. To answer this question, place cell activity of hippocampal CA1 cells was repeatedly recorded at varying intervals or variable task frequency. Long-term tracking of neural activity revealed that overlap of place cell population was independent of the number of tasks performed per unit time, but it was dependent on the duration between the recording sessions (Fig. 3C). The results suggested that the turnover of active population of place cells can be used

as a time code for memories of spatially identical, but temporally different, events [15]. Interestingly, a recent study indicated that overlap between hippocampal CA1 cell ensembles activated by two distinct contexts is greater when the animals are experienced within a day than when separated by longer intervals [14,17]. These findings suggested that the dynamics of CA1 ensembles can work as a general time code for memories of multiple episodes. The present results do not exclude the possibility that any factors other than time affected the place cell turnover rate. In the present study, I showed frequency of well-trained task did not affect the turnover rate (Fig. 3C). However, not a familiar task but more impressive experience such as exploring novel environment may affect the turnover rate.

The present study also investigated the neural mechanisms of place cell turnover. Hippocampal memory is transient and lasts about 3–4 weeks in mice [31]. This suggests that the neural circuits in the hippocampus are continuously modified [32]. Previous studies have shown that NMDA receptor antagonist blocks the decay of LTP in the perforant path-dentate gyrus synapses and enhances spatial memory retention [28–30], suggesting that place cell turnover is also NMDA receptor-dependent process. In the present study, NMDA receptor blockade of CPP reduced the speed of place cell turnover (Fig. 4A, B). This result indicated that NMDA receptors play an important role in the turnover of CA1 ensembles, and this NMDA receptor-dependent turnover of place cell ensembles may be one of the mechanisms determining the lifetime of hippocampal memory.

Another possible mechanism for the place cell turnover is adult neurogenesis in the hippocampus. New neurons are continuously added to neural circuits in the dentate gyrus [33], and this process has been shown to play a significant role in memory retention. For example, forgetting is associated with increased neurogenesis and mitigated by impaired neurogenesis [34]. Factors affecting neurogenesis such as running, environmental enrichment, or stress may alter

place cell turnover rate [35–37].

Although active population of CA1 place cells dynamically changes over time, the place field is generally stable for days to weeks [14,15]. The present study showed that the fluctuation of the place field location is not affected by elapsed time (Fig. 3E, *Left*), task frequency (Fig. 3E, *Right*), and NMDA receptor blockade (Fig. 4C). This suggested the existence of a mechanism that stabilizes the place field against the continuous synaptic modifications.

Methods

Calcium imaging with a custom wide-field microscope

A custom wide-field microscope for in vivo calcium imaging has been previously described [22] (Fig. 1A). Excitation light was emitted from a blue LED (LXK2-PB14-P00; Lumileds, Aachen, Germany). The light passed through an excitation filter (FF480/40-25; Semrock, Rochester, NY) and then reflected by a dichroic mirror (FF506-Di02-25x36; Semrock) onto the tissue through an objective lens (LUCPlan FLN20/0.45; Olympus, Tokyo, Japan). Fluorescent emissions collected by the objective lens were passed through the dichroic mirror and an emission filter (FF535/50-25; Semrock). The fluorescence image, focused by a tube lens (Nikkor 50 mm f/1.8D, Nikon, Tokyo, Japan), was captured by a CMOS camera (FL3-U3-13S2M-CS, FLIR Systems, Willsonville, OR). The optical axis of the microscope was angled at 10 degrees to be perpendicular to the pyramidal cell layer of the CA1 hippocampal region (Fig. 1B).

Animals and surgery

All animal care and use was in accordance with the protocols approved by Hokkaido University

institutional animal care and use committee (project license number: 16-0042). Adult male C57BL/6J mice (10–16 weeks old) were anesthetized using isoflurane and then injected 0.1 mg/kg buprenorphine. The skull was exposed, and a small hole (<0.5 mm) was made over the right hemisphere (1.5 mm lateral to the midline, 2.3 mm posterior to the bregma). AAV1-syn-GCaMP6f-WPRE (University of Pennsylvania vector core) was diluted to 5×10^{12} particles/mL in phosphate-buffered saline, and 150 nL was injected into CA1 (1.2 mm ventral from the brain surface). One week after the viral injection, the animals were anesthetized and a 2.8 mm diameter craniotomy was performed. The dura was removed, and the underlying cortex was aspirated. A stainless-steel cannula (2.76 mm outer diameter, 2.40 mm inner diameter, 1.5 mm height) covered by a glass coverslip (0.12 mm thickness) was inserted over the dorsal CA1. A titanium head plate (25 mm × 10 mm, 1 mm thickness) and the skull were glued with dental cement (Shofu, Kyoto, Japan).

Virtual reality system

The VR system has been previously described [22] (Fig. 1A, 2A). Mice ran along a virtual linear track (1.8 m long) and received a small sugar water reward (4 µl) in an unmarked reward zone (1.5 m from the start point of the track) (Fig. 1D). Once the mice reached the end of the track, they were teleported back to the start of the track.

Behavioral training

At least two weeks after the cranial window implantation, the mice underwent water restriction (2 mL per day), and training in the virtual linear track (10- or 15-min session per day, five days per week) began. After 3–4 weeks of training, mice achieving high performance levels (>10 rewards per single 10 min session) were used for the recording session.

Pharmacology

Mice received intraperitoneal injection of either a saline or 10 mg/kg R-CPP (Tocris, Bristol, UK) after the first recording session and daily thereafter for two days (Fig. 4A).

Imaging session

The excitation light intensity was approximately 0.04 mW/mm^2. Images were captured using FlyCapture2 software (FLIR Systems, Willsonville, OR) at 10 Hz for 10 min. Calcium activity was recorded from19 imaging sites in 16 mice for the long-term imaging experiment (Fig. 3) and from 13 imaging sites in 13 mice for the CPP experiment (Fig. 4). Recordings with a low image quality (blurry image or inconsistent focal plane throughout the experiment) were discarded.

Image processing

ImageJ1.49q (National Institute of Health) and MATLAB 2013a (Mathworks, Natick, MA) were used for all analyses. Fluorescent images were downsampled by a factor of 4. Then lateral displacements of the brain were corrected by image translation using TurboReg [38]. An averaged image of the entire frame was used as a reference for image alignment. Spatial filters corresponding to individual cells were identified using a PCA- and ICA-based algorithm (Cellsort 1.0) (Mukamel et al., 2009). To select spatial filters that follow a typical cell structure, contour of half maximum intensity was calculated, and filters whose area of contour was smaller than 20 pixels or larger than 300 pixels or whose circularity of contour was smaller than 0.7 were discarded.

Detection of Calcium transients

Ca^{2+} activity was determined by applying the spatial filters to the time-lapse image. The Ca^{2+} transients were identified by searching each trace for the local maxima that had a peak amplitude of more than 3× standard deviation from the baseline (defined as the average of the trace calculated across the entire sessions) (Fig. 2B).

Registration of cells across sessions

The threshold spatial filters of all cells from each session were mapped onto a single image. Subsequently, the other filters were aligned to the first day's image via affine transform using TurboReg. Following the alignment across all sessions, cell pairs with a centroid distance <7.8 μm were registered as the same neuron.

Place fields

To analyze place fields, calcium events occurring when the animal's velocity was less than 1 cm/s were filtered out to eliminate nonspecific activity at rest. The number of calcium transients in each bin was divided by the total occupancy time of the mouse in the bin, and then a Gaussian smoothing filter was applied (σ = 2 cm). The number of bins in which a place field had a value greater than 50% of its maximum calcium event rate determined its width. The position of the place field was defined as its centroid.

For each cell's place field, the mutual information between calcium transients and the mouse's location was calculated [39]. To assess the significance of spatial selectivity, Monte Carlo *P* values were calculated. A total of 1,000 distinct shuffles of the calcium transient times were performed, and the mutual information for each shuffle was calculated. The *P* value was defined

as the fraction of the shuffles that exceeded the mutual information of the cell. Cells with $P < 0.05$ were considered place cells.

Statistical analysis

Statistical analysis was performed using GraphPad Prism 5 (GraphPad Software, La Jolla, CA, USA) and MATLAB 2013a. Data were first tested for normality with Shapiro–Wilk test and for homogeneity of variance with Bartlett's test or the *F* test.

Normally distributed data with equal variance were compared with paired/unpaired Student's *t* test or one-way repeated measures ANOVA followed by Tukey post hoc comparisons, as stated in the figure legends. If the data did not meet the assumption of parametric tests, non-parametric tests (Mann–Whitney *U* test, Wilcoxon signed-rank test, or Friedman's test) were used. Statistical significance was set at $P < 0.05$ for all statistical analyses.

References

1. Tulving, E. Episodic Memory: From Mind to Brain. *Annu. Rev. Psychol.* **53,** 1–25 (2002).
2. Scoville, W. B. & Milner, B. Loss of recent memory after bilateral hippocampal lesions. *J. Neurol. Neurosurg. Psychiatry* **20,** 11–21 (1957).
3. Rolls, E. T. A computational theory of episodic memory formation in the hippocampus. *Behav. Brain Res.* **215,** 180–196 (2010).
4. Tulving, E. & Markowitsch, H. J. Episodic and declarative memory: role of the hippocampus. *Hippocampus* **8,** 198–204 (1998).
5. Allen, T. A. & Fortin, N. J. The evolution of episodic memory. *Proc. Natl. Acad. Sci. U. S. A.* **110 Suppl 2,** 10379–86 (2013).

6. O'Keefe, J. & Dostrovsky, J. The hippocampus as a spatial map. Preliminary evidence from unit activity in the freely-moving rat. *Brain Res* **34,** 171–175 (1971).

7. O'Keefe, J. & Nadel, L. *The hippocampus as a cognitive map*. (Oxford University Press, 1978).

8. Moser, M.-B., Rowland, D. C. & Moser, E. I. Place Cells, Grid Cells, and Memory. *Cold Spring Harb. Perspect. Biol.* **7,** a021808 (2015).

9. MacDonald, C. J., Lepage, K. Q., Eden, U. T. & Eichenbaum, H. Hippocampal 'time cells' bridge the gap in memory for discontiguous events. *Neuron* **71,** 737–749 (2011).

10. Eichenbaum, H. Time cells in the hippocampus: a new dimension for mapping memories. *Nat. Rev. Neurosci.* **15,** 732–744 (2014).

11. Pastalkova, E., Itskov, V., Amarasingham, A. & Buzsaki, G. Internally Generated Cell Assembly Sequences in the Rat Hippocampus. *Science (80-.).* **321,** 1322–1327 (2008).

12. Mankin, E. A. *et al.* Neuronal code for extended time in the hippocampus. *Proc Natl Acad Sci U S A* **109,** 19462–19467 (2012).

13. Mankin, E. A., Diehl, G. W., Sparks, F. T., Leutgeb, S. & Leutgeb, J. K. Hippocampal CA2 Activity Patterns Change over Time to a Larger Extent than between Spatial Contexts. *Neuron* **85,** 190–202 (2015).

14. Rubin, A., Geva, N., Sheintuch, L. & Ziv, Y. Hippocampal ensemble dynamics timestamp events in long-term memory. *Elife* **4,** 1–16 (2015).

15. Ziv, Y. *et al.* Long-term dynamics of CA1 hippocampal place codes. *Nat Neurosci* **16,** 264–266 (2013).

16. Manns, J. R., Howard, M. W., Eichenbaum, H., Moser, E. I. & Moser, M. B. Gradual changes in hippocampal activity support remembering the order of events. *Neuron* **56,** 530–40 (2007).

17. Cai, D. J. *et al.* A shared neural ensemble links distinct contextual memories encoded close in time. *Nature* **534,** 115–118 (2016).

18. Dombeck, D. A., Khabbaz, A. N., Collman, F., Adelman, T. L. & Tank, D. W. Imaging large-scale neural activity with cellular resolution in awake, mobile mice. *Neuron* **56,** 43–57 (2007).

19. Dombeck, D. A., Harvey, C. D., Tian, L., Looger, L. L. & Tank, D. W. Functional imaging of hippocampal place cells at cellular resolution during virtual navigation. *Nat Neurosci* **13,** 1433–1440 (2010).

20. Holscher, C., Schnee, A., Dahmen, H., Setia, L. & Mallot, H. A. Rats are able to navigate in virtual environments. *J Exp Biol* **208,** 561–569 (2005).

21. Youngstrom, I. A. & Strowbridge, B. W. Visual landmarks facilitate rodent spatial navigation in virtual reality environments. *Learn. Mem.* **19,** 84–90 (2012).

22. Hayashi, Y., Yawata, S., Funabiki, K. & Hikida, T. In vivo calcium imaging from dentate granule cells with wide-field fluorescence microscopy. *PLoS One* **12,** e0180452 (2017).

23. Lever, C., Wills, T., Cacucci, F., Burgess, N. & O'Keefe, J. Long-term plasticity in hippocampal place-cell representation of environmental geometry. *Nature* **416,** 90–94 (2002).

24. Thompson, L. T. & Best, P. J. Long-term stability of the place-field activity of single units recorded from the dorsal hippocampus of freely behaving rats. *Brain Res* **509,** 299–308 (1990).

25. Malenka, R. C. & Nicoll, R. A. NMDA-receptor-dependent synaptic plasticity: multiple forms and mechanisms. *Trends Neurosci* **16,** 521–527 (1993).

26. Steele, R. J. & Morris, R. G. Delay-dependent impairment of a matching-to-place task

with chronic and intrahippocampal infusion of the NMDA-antagonist D-AP5. *Hippocampus* **9,** 118–136 (1999).

27. Nakazawa, K., McHugh, T. J., Wilson, M. A. & Tonegawa, S. NMDA receptors, place cells and hippocampal spatial memory. *Nat. Rev. Neurosci.* **5,** 361–372 (2004).

28. Villarreal, D. M., Do, V., Haddad, E. & Derrick, B. E. NMDA receptor antagonists sustain LTP and spatial memory: active processes mediate LTP decay. *Nat. Neurosci.* **5,** 48–52 (2002).

29. Sachser, R. M. *et al.* Forgetting of long-term memory requires activation of NMDA receptors, L-type voltage-dependent Ca(2+) channels, and calcineurin. *Sci. Rep.* **6,** 22771 (2016).

30. Shinohara, K. & Hata, T. Post-acquisition hippocampal NMDA receptor blockade sustains retention of spatial reference memory in Morris water maze. *Behav. Brain Res.* **259,** 261–267 (2014).

31. Frankland, P. W. & Bontempi, B. The organization of recent and remote memories. *Nat. Rev. Neurosci.* **6,** 119–130 (2005).

32. Attardo, A., Fitzgerald, J. E. & Schnitzer, M. J. Impermanence of dendritic spines in live adult CA1 hippocampus. *Nature* **523,** 592–596 (2015).

33. Zhao, C., Deng, W. & Gage, F. H. Mechanisms and functional implications of adult neurogenesis. *Cell* **132,** 645–660 (2008).

34. Akers, K. G. *et al.* Hippocampal Neurogenesis Regulates Forgetting During Adulthood and Infancy. *Science (80-.).* **344,** 598–602 (2014).

35. van Praag, H., Kempermann, G. & Gage, F. H. Running increases cell proliferation and neurogenesis in the adult mouse dentate gyrus. *Nat Neurosci* **2,** 266–270 (1999).

36. Kempermann, G., Kuhn, H. G. & Gage, F. H. More hippocampal neurons in adult mice

living in an enriched environment. *Nature* **386,** 493–495 (1997).

37. Gould, E., McEwen, B. S., Tanapat, P., Galea, L. A. & Fuchs, E. Neurogenesis in the dentate gyrus of the adult tree shrew is regulated by psychosocial stress and NMDA receptor activation. *J Neurosci* **17,** 2492–2498 (1997).

38. Thévenaz, P., Ruttimann, U. E. & Unser, M. A pyramid approach to subpixel registration based on intensity. *IEEE Trans. Image Process.* **7,** 27–41 (1998).

39. Skaggs, W. E., McNaughton, B. L., Gothard, K. M. & Markus, E. J. *An information-theoretic approach to deciphering the hippocampal code. Advances in neural information processing systems* **5,** (Morgan Kaufmann, 1993).

Acknowledgments

This work is supported by JSPS KAKENHI grant number 17K19436. The author would like to thank Enago (www.enago.jp) for the English language review.

Competing financial interests

The author declares that there is no conflict of interest.

Figure Legends

Figure 1. Calcium imaging of hippocampal activity in awake, head-restrained mice under VR environment

(A) Simplified schematic representation of the imaging system. The blue line indicates the illumination pathway and the green line indicates the light collection pathway. Illumination light from a blue LED was collected with a condenser lens, passed through an excitation filter, reflected off a dichroic mirror, and irradiated through an objective lens. The fluorescence image

was focused on a CMOS camera. (B) Schematic representation of the experimental setup showing the chronic window implant above CA1. The optical axis of the fluorescence microscope was angled at 10 degrees. (C) View from the start point of the virtual linear track. (D) Top view of the track.

Figure 2. Hippocampal activity during the VR task

(A) Sample image of mean fluorescence during an imaging session. Contours of cells extracted from the fluorescent imaging movie are shown in orange circles (236 cells). (B) Relative fluorescence changes (dF/F) for 12 cells. Identified calcium transients are shown as red dots. (C) Representative CA1 cell activity. *Left*, place cell (mutual information = 1.7, Monte Carlo *P* value = 0.000); *Right*, nonspecific cell (mutual information = 0.13, Monte Carlo *P* value = 0.48). The position of the mouse along the virtual track is shown by the blue line. Identified calcium activities during running are shown with red asterisks, and those during rest are shown with black asterisks.

Figure 3. Long-term imaging of CA1 place cell activity

(A) Experimental timeline. After at least three weeks of pre-training, a series of four recording sessions was conducted on days 1–4; another series of four recording sessions was conducted on days 7–10. (B) Place field maps for the same cells on multiple days of the recording session, arranged by their centroid position on the virtual linear track. (C) If a cell had a statistically significant place field in one session, the odds that it had a place field in a subsequent session were displayed as recurrence probability. *Left*, recurrence probability for sessions with a one-day interval (recurrence between days 1 and 2, 2 and 3, 3 and 4, 7 and 8, 8 and 9, 9 and 10) versus that for sessions with a three-day interval (between days 4 and 7) were plotted.

Significance was evaluated by performing an unpaired *t* test (t = 2.9, df = 54, P = 0.0044, n = 48 for 1-day interval, n = 8 for 3 day interval). *Middle*, recurrence probability for adjacent sessions were plotted. Significance was evaluated by one-way repeated measures ANOVA followed by Tukey post hoc test ($F_{6,48}$ = 5.5, P = 0.0003, n = 8). *Right*, recurrence probability for sessions with a three-day interval. Significance was evaluated by one-way repeated measures ANOVA followed by Tukey post hoc test ($F_{2,21}$ = 1.9, P = 0.19, n = 8). (D) Distribution of centroid shifts of place fields between adjacent recording sessions (1-2, 2-3, 3-4, 4-7, 7-8, 8-9, and 9-10). (E) *Left*, centroid shifts of the place fields between adjacent recording sessions. Significance was evaluated by one-way repeated measures ANOVA ($F_{6,48}$ = 1.622, P = 0.17, n = 8). *Right*, centroid shifts between sessions with a three-day interval. Significance was evaluated by one-way repeated measures ANOVA followed by Tukey post hoc test ($F_{2,21}$ = 0.63, P = 0.55, n = 8). Data are shown as mean ± SEM. Asterisks indicate significantly different (*P < 0.05, **P < 0.01, ***P < 0.001; otherwise not significant).

Figure 4. NMDA receptor antagonism reduced turnover of place cells

(A) Experimental timeline. After the pre-training period, two recording sessions were conducted on days 1 and 4. R-CPP was intraperitoneally administrated after the first recording session and daily thereafter for two days. (B) Recurrence probability for the two sessions under saline and R-CPP conditions. Significance was evaluated by Mann–Whitney *U* test (P = 0.032). (C) Centroid shifts of place fields between the two sessions under saline and R-CPP conditions. *Left*, distributions of centroid shifts. *Right*, average centroid shifts. Significance was evaluated by Mann–Whitney *U* test (P = 1.0). Data are shown as mean ± SEM. Asterisks indicate significant differences (*P < 0.05; otherwise not significant).

Fig 1

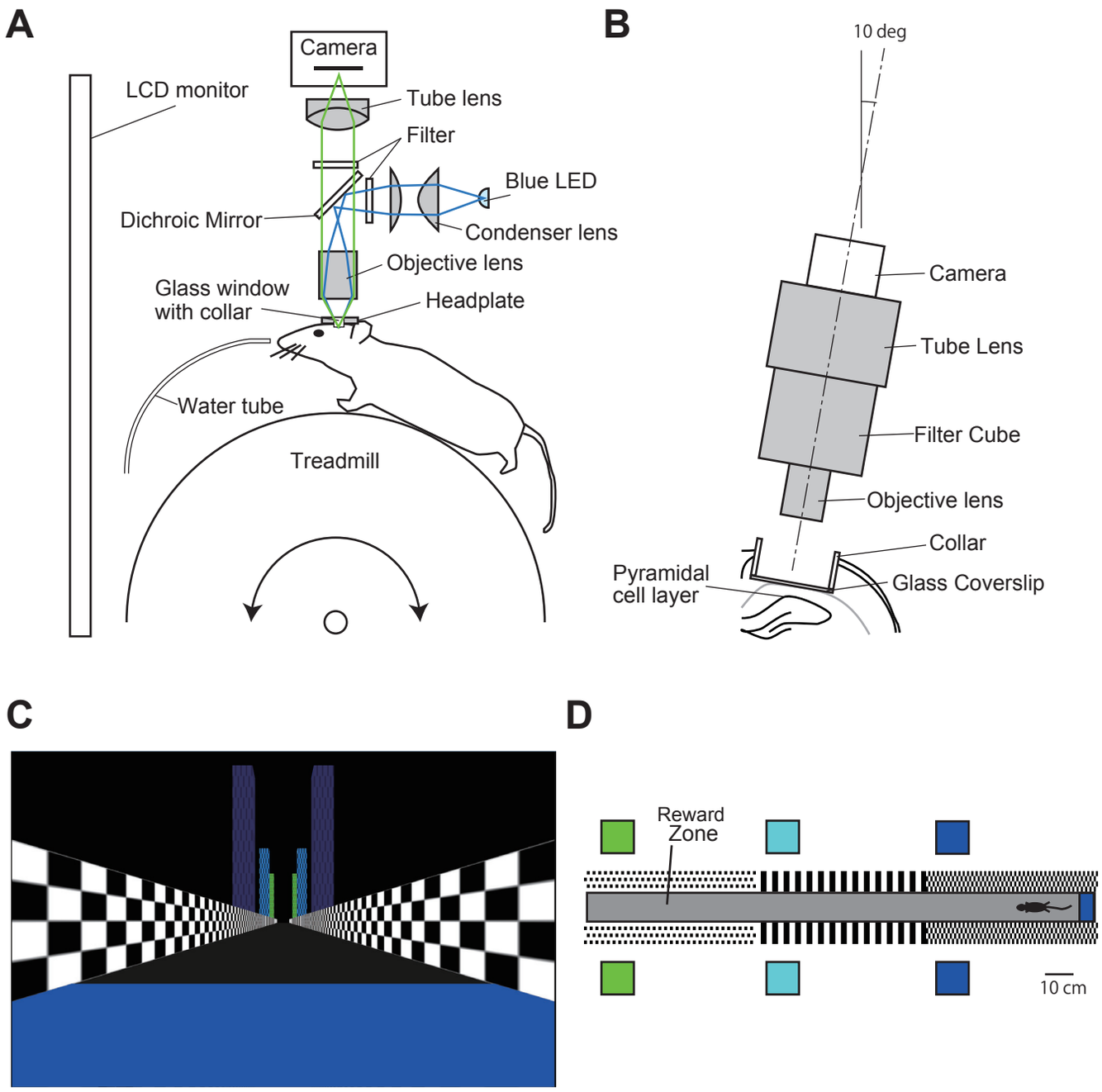
A
Camera
LCD monitor
Tube lens
Filter
Blue LED
Dichroic Mirror
Condenser lens
Objective lens
Glass window
with collar
Headplate
Water tube
Treadmill
B
10 deg
Camera
Tube Lens
Filter Cube
Objective lens
Collar
Pyramidal
cell layer
Glass Coverslip
C
D
Reward
Zone
10 cm

Fig 2

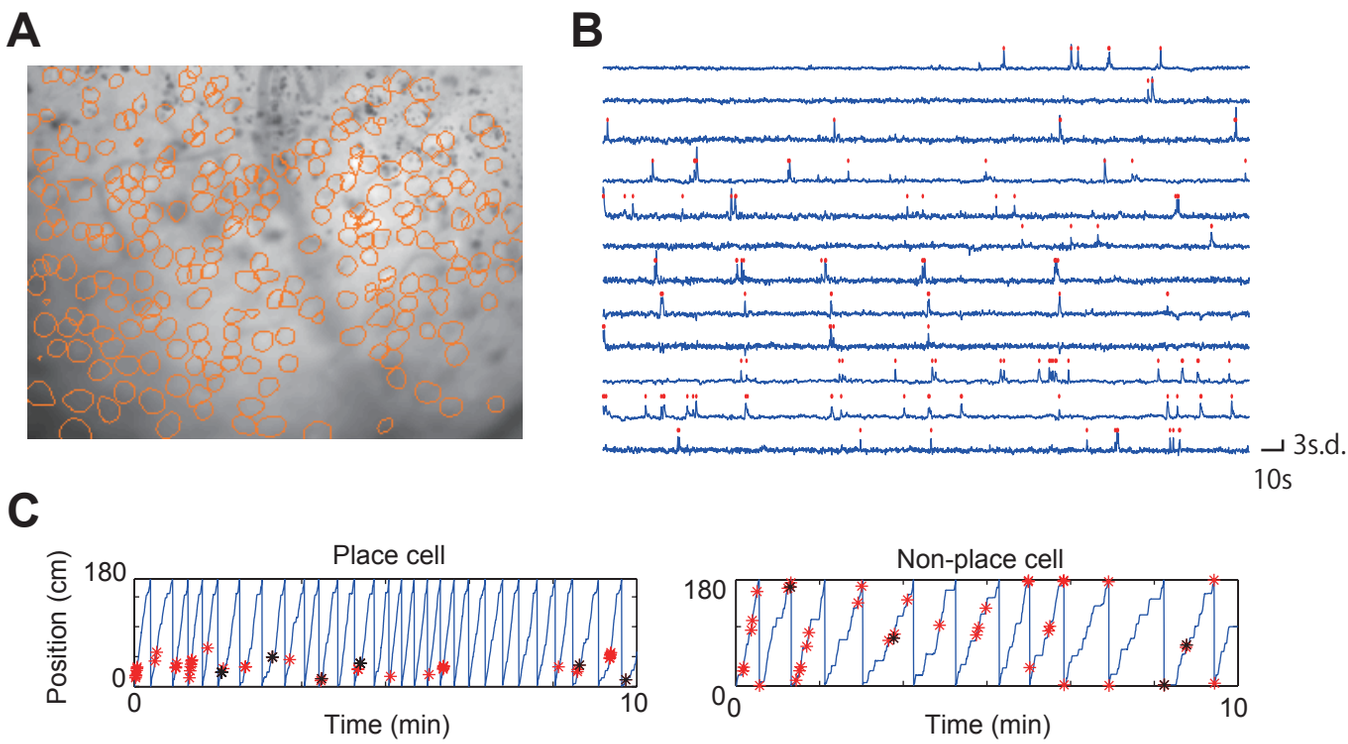
A
B
3s.d.
10s
C
Place cell
Non-place cell
Position (cm)
180
0
0
10
Time (min)
180
0
0
10
Time (min)

Fig 3

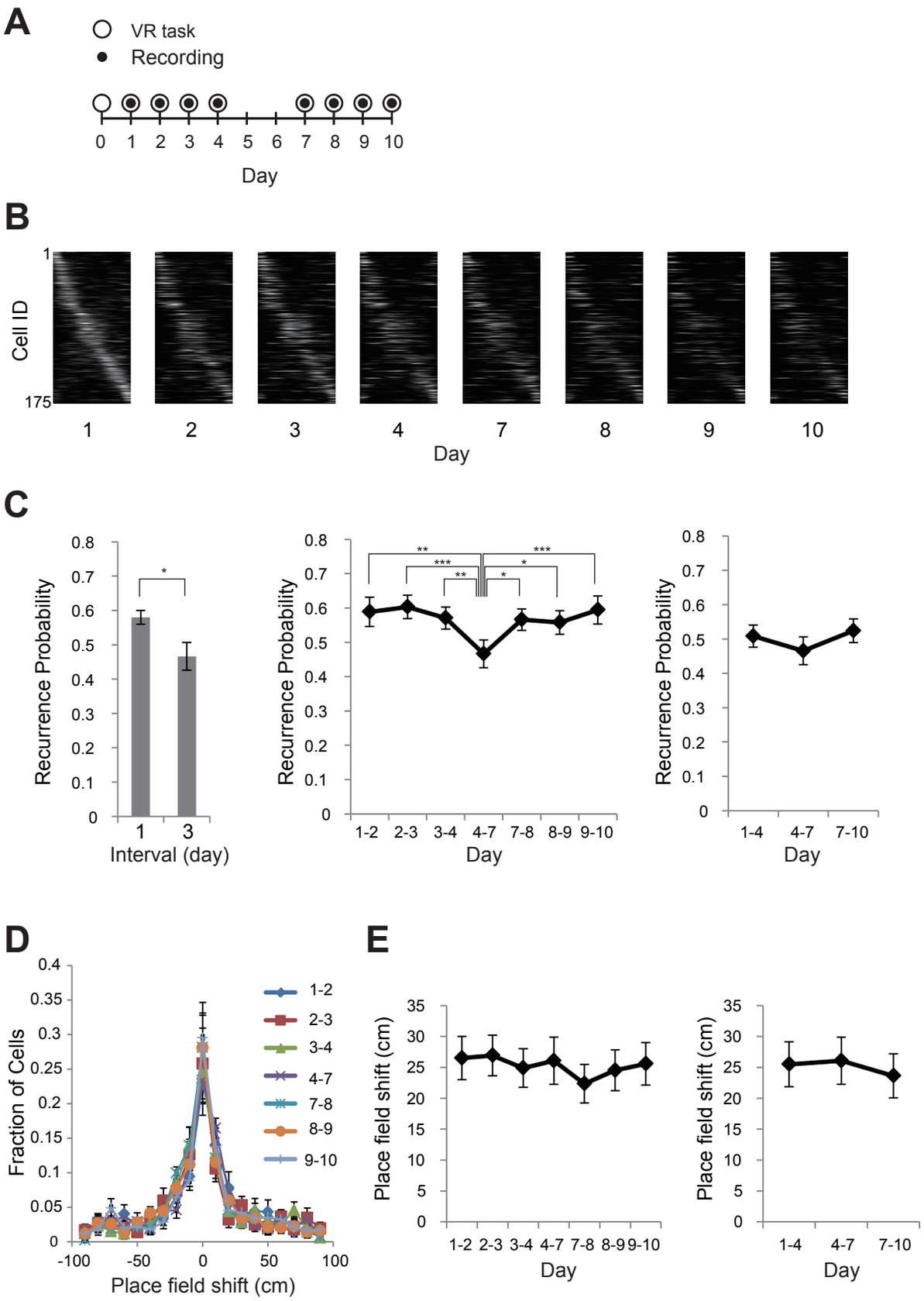
A
VR task
Recording
0 1 2 3 4 5 6 7 8 9 10
Day
B
Cell ID
1
175
1 2 3 4 7 8 9 10
Day
C
Recurrence Probability
Interval (day)
1 3
1-2 2-3 3-4 4-7 7-8 8-9 9-10
Day
1-4 4-7 7-10
Day
D
Fraction of Cells
Place field shift (cm)
1-2
2-3
3-4
4-7
7-8
8-9
9-10
E
Place field shift (cm)
1-2 2-3 3-4 4-7 7-8 8-9 9-10
Day
1-4 4-7 7-10
Day

Fig 4

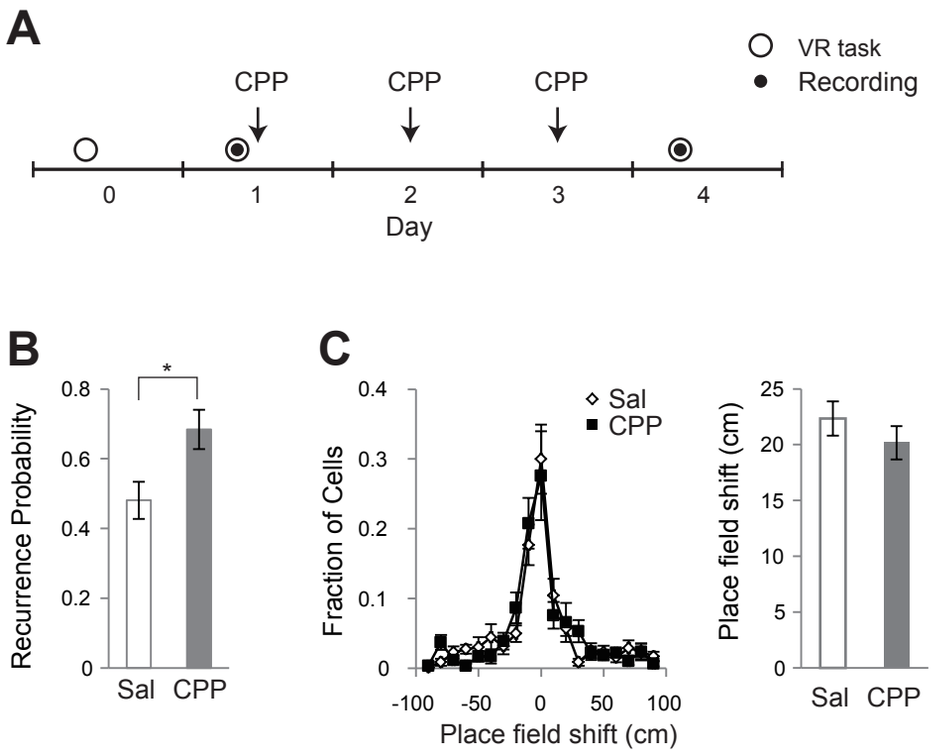
A
VR task
Recording
CPP
CPP
CPP
0
1
2
3
4
Day
B
Recurrence Probability
0.8
0.6
0.4
0.2
0
*
Sal
CPP
C
Fraction of Cells
0.4
0.3
0.2
0.1
0
Sal
CPP
-100
-50
0
50
100
Place field shift (cm)
Place field shift (cm)
25
20
15
10
5
0
Sal
CPP